

Phase diagram of the penetrable square well-model

RICCARDO FANTONI¹, ALEXANDR MALIJEVSKÝ², ANDRÉS SANTOS³ and ACHILLE GIACOMETTI⁴

¹ *National Institute for Theoretical Physics (NITheP) and Institute of Theoretical Physics, Stellenbosch 7600, South Africa*

² *E. Hála Laboratory of Thermodynamics, Institute of Chemical Process Fundamentals of the ASCR, and Department of Physical Chemistry, Institute of Chemical Technology, Prague, 166 28 Praha 6, Czech Republic*

³ *Departamento de Física, Universidad de Extremadura, E-06071 Badajoz, Spain*

⁴ *Dipartimento di Chimica Fisica, Università Ca' Foscari Venezia, S. Marta DD2137, I-30123 Venezia, Italy*

PACS 64.60.De –
 PACS 64.60.Ej –
 PACS 64.70.D– –
 PACS 64.70.Hz –
 PACS 64.70.F– –

Abstract – We study a system formed by soft colloidal spheres attracting each other via a square-well potential, using extensive Monte Carlo simulations of various nature. The softness is implemented through a reduction of the infinite part of the repulsive potential to a finite one. For sufficiently low values of the penetrability parameter we find the system to be Ruelle stable with square-well like behavior. For high values of the penetrability the system is thermodynamically unstable and collapses into an isolated blob formed by a few clusters each containing many overlapping particles. For intermediate values of the penetrability the system has a rich phase diagram with a partial lack of thermodynamic consistency.

Pair effective interactions in soft condensed matter physics can be of various nature and one can often find real systems whose interaction is bounded at small separations as, for instance, in the case of star and chain polymers [1]. In this case, paradigmatic models, such as square-well (SW) fluids, that have been rather successful in predicting thermo-physical properties of simple liquids, are no longer useful. Instead, different minimal models accounting for the boundness of the potential have to be considered, the Gaussian core model [2] and the penetrable-sphere (PS) model [3–5] being well studied examples. More recently, the penetrable square-well (PSW) fluid has been added to this category [6–9] with the aim of including the existence of attractive effective potentials. The PSW model is obtained from the SW potential by reducing to a finite value the infinite repulsion at short range,

$$\phi_{\text{PSW}}(r) = \begin{cases} \epsilon_r, & r \leq \sigma, \\ -\epsilon_a, & \sigma < r \leq \sigma + \Delta, \\ 0, & r > \sigma + \Delta, \end{cases} \quad (1)$$

where ϵ_r and ϵ_a are two positive energies accounting for the repulsive and attractive parts of the potential, respectively, Δ is the width of the attractive square well, and

σ is the width of the repulsive barrier. For $\epsilon_r \rightarrow \infty$ one recovers the SW model, while for $\Delta = 0$ or $\epsilon_a = 0$ one recovers the PS model.

For finite ϵ_a , ϵ_a/ϵ_r is a measure of the penetrability of the barrier and we shall refer to ϵ_a/ϵ_r as the penetrability ratio. PSW pair potentials can be obtained as effective potentials for instance in polymer mixtures [10,11]. While in the majority of the cases the well depth ϵ_a is much smaller than the repulsive barrier ϵ_r (low penetrability limit) this mesoscopic objects are highly sensitive to external conditions (e.g. quality of the solvent) and may thus in principle exhibit higher values of the penetrability ratio ϵ_a/ϵ_r .

It is well known that three-dimensional SW fluids exhibit a fluid-fluid phase transition for any width of the attractive square well [12–16], the liquid phase becoming metastable against the formation of the solid for a sufficiently narrow well [15]. It is also well established that in the PS fluid (that lacking an attractive component in the pair potential cannot have a fluid-fluid transition) an increase of the density leads to the formation of clusters of overlapping particles arranged in an ordered crystalline phase [3,17–19].

While the novel features appearing even in the one-

dimensional case have been studied in some details [6–9], no analysis regarding the influence of penetrability and attractiveness on the phase behavior of PSW fluids have been reported, so far, in three dimensions. The present paper aims to fill this vacancy.

A system is defined to be Ruelle stable when the total potential energy U_N for a system of N particles satisfies the condition $U_N \geq -NB$ where B is a finite positive constant [20, 21]. In Ref. [8] we proved that in the one-dimensional case the PSW model is Ruelle stable if $\epsilon_a/\epsilon_r < 1/2(\ell + 1)$, where ℓ is the integer part of Δ/σ . This result can be extended to any dimensionality d by the following arguments. The configuration which minimizes the energy of N particles interacting via the PSW potential is realized when M closed packed clusters, each consisting of $s = N/M$ particles collapsed into one point, are distributed such that the distance between centers of two neighbor clusters is σ . In such a configuration, all the particles of the same cluster interact repulsively, so the repulsive contribution to the total potential energy is $\epsilon_r Ms(s - 1)/2$. In addition, the particles of a given cluster interact attractively with all the particles of those f_Δ clusters within a distance smaller than $\sigma + \Delta$. In the two-dimensional case, $f_\Delta = 6$ and 12 if $\Delta/\sigma < \sqrt{3} - 1$ and $\sqrt{3} - 1 < \Delta/\sigma < 1$, respectively. For $d = 3$, the case we are interested in, one has $f_\Delta = 12, 18,$ and 42 if $\Delta/\sigma < \sqrt{2} - 1$, $\sqrt{2} - 1 < \Delta/\sigma < \sqrt{3} - 1$, and $\sqrt{3} - 1 < \Delta/\sigma < 1$, respectively. The attractive contribution to the total potential energy is thus $-\epsilon_a(M/2)[f_\Delta - b_\Delta(M)]s^2$, where $b_\Delta(M)$ accounts for a reduction of the actual number of clusters interacting attractively, due to boundary effects. This quantity has the properties $b_\Delta(M) < f_\Delta$, $b_\Delta(1) = f_\Delta$, and $\lim_{M \rightarrow \infty} b_\Delta(M) = 0$. For instance, in the two-dimensional case with $\Delta/\sigma < \sqrt{3} - 1$ one has $b_\Delta(M) = 2(4\sqrt{M} - 1)/M$. Therefore, the total potential energy is

$$\frac{U_N(M)}{N\epsilon_r} = -\frac{1}{2} + \frac{N}{2M}F(M), \quad (2)$$

where $F(M) \equiv (\epsilon_a/\epsilon_r)b_\Delta(M) + (1 - f_\Delta\epsilon_a/\epsilon_r)$. If $\epsilon_a/\epsilon_r < 1/f_\Delta$, $F(M)$ is positive definite, so $U_N(M)/N$ has a lower bound and the system is stable in the thermodynamic limit. On the other hand, if $\epsilon_a/\epsilon_r > 1/f_\Delta$, one has $F(1) = 1$ but $\lim_{M \rightarrow \infty} F(M) = -(f_\Delta\epsilon_a/\epsilon_r - 1) < 0$. In that case, there must exist a certain *finite* value $M = M_0$ such that $F(M) < 0$ for $M > M_0$. As a consequence, in those configurations with $M > M_0$, $U_N(M)/N$ has no lower bound in the limit $N \rightarrow \infty$ and thus the system may be unstable.

We have performed an extensive analysis of the vapor-liquid phase transition of the system using Gibbs Ensemble Monte Carlo (GEMC) simulations [22–26], starting from the corresponding SW fluid condition and gradually increasing the penetrability ratio ϵ_a/ϵ_r until the transition disappears. A total number of $N = 512$ particles with $2N$ particle random displacement, $N/10$ volume changes, and N particle swap moves between the gas and the liquid box, on average per cycle, were considered. We find that

for any given width $\Delta/\sigma < 1$ of the well, there is a limit value of the penetrability ratio ϵ_a/ϵ_r above which no fluid-fluid phase transition is observed. This is depicted in Fig. 1 where it can be observed that (for $\Delta/\sigma < 1$) this line lies outside the Ruelle stable region $\epsilon_a/\epsilon_r < 1/f_\Delta$.

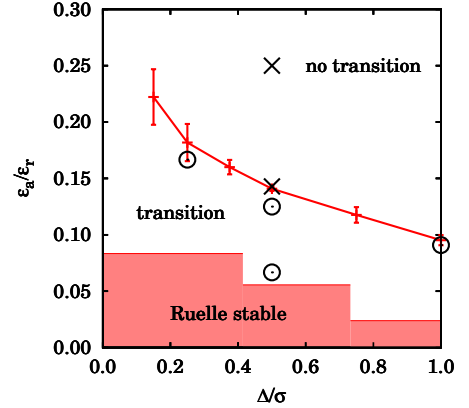


Fig. 1: Plot of the penetrability ratio ϵ_a/ϵ_r as a function of Δ/σ . The displayed line separates the parameter region where the PSW model admits a fluid-fluid phase transition from that where it does not. The highlighted region ($\epsilon_a/\epsilon_r \leq 1/12$ for $\Delta/\sigma < \sqrt{2} - 1$, $\epsilon_a/\epsilon_r \leq 1/18$ for $\sqrt{2} - 1 < \Delta/\sigma < \sqrt{3} - 1$, and $\epsilon_a/\epsilon_r \leq 1/42$ for $\sqrt{3} - 1 < \Delta/\sigma < 1$) shows where the model is expected to be thermodynamically stable in the sense of Ruelle for any thermodynamic state. The SW model falls on the horizontal axis ($\epsilon_a/\epsilon_r \rightarrow 0$) and its fluid-fluid transition is expected to be metastable against the freezing transition for $\Delta/\sigma \lesssim 0.25$ [15]. The circles are the points chosen for the calculation of the coexistence lines (see Figs. 2 and 5). The crosses are the points chosen for the determination of the boundary between extensive and non-extensive phases (see Fig. 3).

It is instructive to analyze the detailed form of the coexistence curves below (but close to) the limit line of Fig. 1. This is presented in Fig. 2. We have explicitly checked that our code reproduces completely the results of Vega et al. [12] for the SW model. Following standard procedures [12] we fitted the GEMC points, near the critical point using the law of rectilinear diameters $(\rho_l + \rho_g)/2 = \rho_c + A(T_c - T)$ where ρ_l (ρ_g) is the density of the liquid (gas) phase, ρ_c is the critical density, and T_c is the critical temperature. Furthermore, the temperature dependence of the density difference of the coexisting phases is fitted to the scaling law $\rho_l - \rho_g = B(T_c - T)^\beta$ where $\beta = 0.32$ is the critical exponent for the three-dimensional Ising model. The amplitudes A and B were determined from the fit. In the state points above the limit line of Fig. 1 we have considered temperatures below the critical temperature of the corresponding SW system. The disappearance of the fluid-fluid transition is signaled by the evolution towards an empty gas box and a clustered phase in the liquid box.

As discussed, the PSW fluid is thermodynamically Ru-

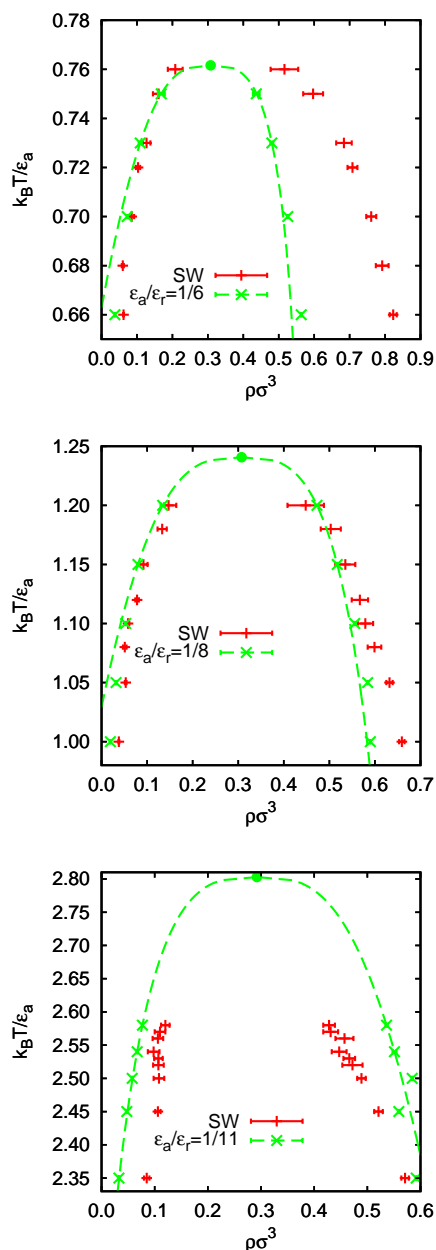


Fig. 2: Fluid-fluid coexistence line. The solid circle represents the critical point (ρ_c, T_c) . In the top panel, for $\Delta/\sigma = 0.25$ and $\epsilon_a/\epsilon_r = 1/6$, one has $\rho_c \sigma^3 = 0.307$ and $k_B T_c/\epsilon_a = 0.762$; in the middle panel, below the limit penetrability, for $\Delta/\sigma = 0.5$ and $\epsilon_a/\epsilon_r = 1/8$, one has $\rho_c \sigma^3 = 0.307$ and $k_B T_c/\epsilon_a = 1.241$; and in the bottom panel for $\Delta/\sigma = 1.0$ and $\epsilon_a/\epsilon_r = 1/11$, one has $\rho_c \sigma^3 = 0.292$ and $k_B T_c/\epsilon_a = 2.803$. The lines are the result of the fit with the law of rectilinear diameters. The SW results are the ones of Vega et al. [12]

elle stable when $\epsilon_a/\epsilon_r < 1/f_\Delta$ for all values of the thermodynamic parameters. For $\epsilon_a/\epsilon_r > 1/f_\Delta$ the system is either extensive or non-extensive depending on temperature and density. For a given density, one could then expect that there exists a certain temperature $T_{\text{inst}}(\rho)$,

such that the system is metastable if $T > T_{\text{inst}}$ and unstable if $T < T_{\text{inst}}$. We determined the metastable/unstable crossover by performing NVT Monte Carlo simulations with $N = 512$ particles initially uniformly distributed within the simulation box. Figure 3 reports the results in the reduced temperature-density plane for $\Delta/\sigma = 0.5$ and for two selected penetrability ratios $\epsilon_a/\epsilon_r = 1/7$ and $1/4$, the first one lying exactly just above the limit line of Fig. 1 while the second deep in the non-transition region. We worked with constant size moves (instead of fixing the acceptance ratios) during the simulation run, choosing the move size of 0.15 in units of the the simulation box side. A

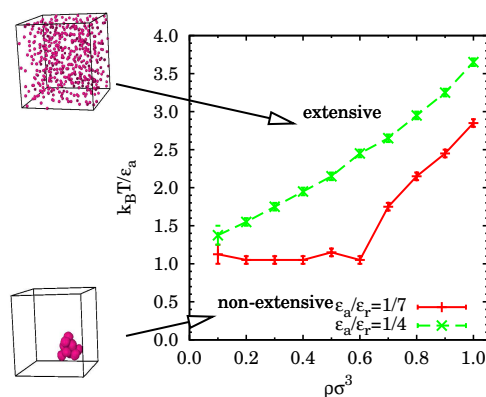


Fig. 3: Regions of the phase diagram where the PSW fluid, with $\Delta/\sigma = 0.5$ and two different values of ϵ_a/ϵ_r , is found to be extensive or non-extensive (here we used $N = 512$ particles). The left shows representative snapshots in the two regions. The instability line corresponding to the higher penetrability case (dashed line) lies above the one corresponding to lower penetrability (continuous line).

crucial point in the above numerical analysis is the identification of the onset of the instability. Clearly the physical origin of this instability stems from the fact that the attractive contribution increases unbounded compared to the repulsive one and particles tend to lump up into clusters of multiply overlapping particles (“blob”). Hence the energy can no longer scale linearly with the total number of particles N and the thermodynamic limit is not well defined (non-extensivity). We define a cluster in the following way. Two particles belong to the same cluster if there is a path connecting them, where we are allowed to move on a path going from one particle to another if the centers of the two particles are at a distance less than σ .

The state points belonging to the unstable region are characterized by a sudden drop of the internal energy and of the acceptance ratios at some points in the system evolution during the MC simulation. Representative snapshots show that a blob structure has nucleated around a certain point and occupies only a part of the simulation box with a few clusters. The number of clusters decreases as one moves away from the boundary line found in Fig.

3 towards lower temperatures. Upon increasing ϵ_a/ϵ_r the number of clusters decreases and the number of particles per cluster increases. We assume a state to be metastable if the energy does not undergo the transition after $10^7 N$ single particle moves. The fluid-fluid transition above the limit penetrability line of Fig. 1 is not possible because the non-extensive phase shows up before the critical point is reached.

The boundary line of Fig. 3 is robust with respect to the size of the system, provided that a sufficiently large size ($N \geq 512$) is chosen. When the number of particles in the simulation goes below the number of clusters which would form in the non-extensive phase the system seems to remain extensive. For instance, with $N = 1024$ particles we obtained under the $\epsilon_a/\epsilon_r = 1/7$, $\Delta/\sigma = 0.5$ conditions a threshold temperature $k_B T/\epsilon_a \approx 1.15$ for $\rho\sigma^3 = 0.4$ and 2.25 for $\rho\sigma^3 = 0.8$, which are close to the values obtained with $N = 512$ particles.

There is an apparent hysteresis in forming and melting the non-extensive phase. For example when $\epsilon_a/\epsilon_r = 1/7$, $\Delta/\sigma = 0.5$, and $\rho\sigma^3 = 1.0$ the non-extensive phase starts forming when cooling down to $k_B T/\epsilon_a = 2.75$. Upon increasing the temperature again, we observed a melting transition at significantly higher temperatures ($k_B T/\epsilon_a \gtrsim 4$). We also found the hysteresis to be size dependent; in the same state for $\rho\sigma^3 = 0.6$ the melting temperatures are $k_B T/\epsilon_a \approx 2.5$ for $N = 256$, $k_B T/\epsilon_a \approx 4.5$ for $N = 512$, and $k_B T/\epsilon_a \approx 6.5$ for $N = 1024$. This suggests that the extensive phase in Fig. 3 is actually metastable with respect to the non-extensive phase in the thermodynamic limit. However the metastable phase can be stabilized by taking the size of the system finite. In addition we cannot exclude, a priori, the possibility of a true extensive stable phase as it is not prevented by the Ruelle criterion. We note that the size dependence of the hysteresis in the melting could be attributed to the fact that the blob occupies only part of the simulation box and therefore a surface term has a rather high impact on the melting temperature.

A convenient way to characterize the structure of the fluid is to consider the radial distribution function $g(r)$. This is depicted in Fig. 4 for the cases $\Delta/\sigma = 0.5$, $k_B T/\epsilon_a = 1.20$, and $\rho\sigma^3 = 0.7$ at $\epsilon_a/\epsilon_r = 1/8$ and $\epsilon_a/\epsilon_r = 1/7$. The latter case is in the non-extensive region, according to Fig. 3. We can clearly see that there is a dramatic change in the structural properties of the PSW liquid. In the non-extensive case, $\epsilon_a/\epsilon_r = 1/7$, the radial distribution function grows a huge peak at $r = 0$ and decays to zero after the first few peaks, which suggests clustering and confinement of the system.

In order to study the solid phase of the PSW model below the limit penetrability we employed isothermal-isobaric (NPT) MC simulations. A typical run would consist of 10^8 steps (particle moves or volume moves) with an equilibration time of 10^7 steps. We used 108 particles and adjusted the particle moves to have acceptance ratios of ≈ 0.5 and volume changes to have acceptance ratios

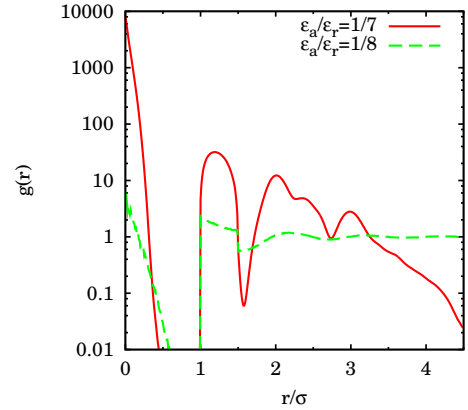


Fig. 4: Radial distribution function for the PSW model at $\Delta/\sigma = 0.5$, $k_B T/\epsilon_a = 1.20$, and $\rho\sigma^3 = 0.7$ for two different values of the penetrability ratio ϵ_a/ϵ_r .

of ≈ 0.1 . Here we only consider the case of PSW with $\Delta/\sigma = 0.5$ and $\epsilon_a/\epsilon_r = 1/8$ and $1/15$.

For the SW system with a width $\Delta/\sigma = 0.5$ the critical point is known to be at $k_B T_c/\epsilon_a = 1.23$ and $\rho_c\sigma^3 = 0.309$, its triple point being at $k_B T_t/\epsilon_a = 0.508$, $P_t\sigma^3/\epsilon_a = 0.00003$, $\rho_l\sigma^3 = 0.835$, and $\rho_s\sigma^3 = 1.28$ [15]. No solid stable phase was found in Ref. [15] for temperatures above the triple point, meaning that the melting curve in the pressure-temperature phase diagram is almost vertical. On the other hand, the phase diagram of the PSW fluid with the same well width and a value of $\epsilon_a/\epsilon_r = 1/8$, just below the limit line of Fig. 1, shows that the melting curve has a smooth positive slope in the pressure-temperature phase diagram. In order to establish this, we used NPT simulations to follow the $k_B T/\epsilon_a = 1$ isotherm. From Fig. 5 we can clearly see the jumps in density corresponding to the gas-liquid and to the liquid-solid coexistence regions. The presence of a solid phase can be checked by computing the Q_6 order parameter [27], calculated for the center of mass of individual clusters, that in the present case turns out to be $Q_6 \approx 0.35$. The crystal structure is triclinic with a unit cell with $a = b = c = \sigma$ and $\alpha = \beta = \pi/3$ and $\gamma = \cos^{-1}(1/4)$. There are possibly other solid-solid coexistence regions at higher pressures. Moreover the relaxation time of the MC run in the solid region is an order of magnitude higher than the one in the liquid region.

We also run at the same temperature a set of simulations for the PSW fluid with $\epsilon_a/\epsilon_r = 1/15$. The results (see Fig. 5) showed no indication of a stable solid, in agreement with the fact that at this very low value of the penetrability ratio the system is SW-like.

A peculiarity of the PSW in the region below the limit penetrability of Fig. 1, but not in the Ruelle stability region, is a violation of the Clausius-Clapeyron equation [28] along the liquid-solid coexistence curve, what represents a partial lack of thermodynamic consistency

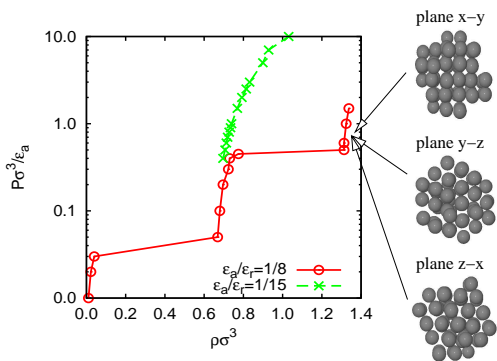


Fig. 5: Isotherm $k_B T/\epsilon_a = 1$ for the PSW system with $\Delta/\sigma = 0.5$ and $\epsilon_a/\epsilon_r = 1/8$ and $\epsilon_a/\epsilon_r = 1/15$, as obtained from NPT MC simulation with $N = 108$ particles. The pressure axis is in logarithmic scale. The right shows snapshots of the centers of mass of the clusters in the solid.

In the intermediate penetrability case (i.e., above Ruelle's threshold but below the limit penetrability), the observed crystal structure is made of clusters of overlapping particles (rarely more than two) located at the sites of a regular crystal lattice. It is precisely this additional degree of penetrability, not present in the SW system, that allows for the coexistence of the liquid and the solid at not excessively large pressures. In this respect qualitative arguments along the lines suggested in Ref. [19] could be useful.

In conclusion, we have studied the phase diagram of the three-dimensional PSW system. This model is Ruelle stable for $\epsilon_a/\epsilon_r < 1/f_\Delta$. For $\epsilon_a/\epsilon_r > 1/f_\Delta$ is either metastable or unstable (non-extensive), depending on the values of temperature and density, as shown in Fig. 3. The instability is indicated by the collapse of the system in a confined blob made up of a few clusters of several overlapping particles. Moreover, the gas-liquid phase transition disappears, as shown in Fig. 1.

For the metastable fluid near the limit penetrability line of Fig. 1 we determined the phase diagram comparing it with the corresponding SW case. We determined how the gas-liquid coexistence curves are modified by the presence of penetrability (see Fig. 2) and discussed the main features of the phase diagram, including the solid phase, for $\Delta/\sigma = 0.5$.

For the liquid-solid coexistence curves we generally found that the solid density increases with respect to the corresponding SW case, as expected, due to the formation of clusters of overlapping particles in the crystal sites. For $\Delta/\sigma = 0.5$ the PSW model with a sufficient penetrability to have a metastable system, but not a Ruelle stable one, has a melting curve with a positive slope in the pressure-temperature phase diagram with a violation of the Clausius-Clapeyron thermodynamic equation, thus confirming the metastable character of the phases. For sufficient low penetrability the system is in the Ruelle sta-

ble region, and behaves as the corresponding SW model.

In summary, by experimentally tuning the repulsive barrier relative to the well depth one could observe (a) stable phases resembling those of a normal fluid, (b) metastable phases with fluid-fluid and fluid-solid coexistence, or (c) the collapse of the system to a small region.

* * *

We thank Tatyana Zykova-Timan and Bianca M. Mladek for enlightening discussions and useful suggestions. The support of PRIN-COFIN 2007B58EAB, FEDER FIS2010-16587 (Ministerio de Ciencia e Innovación), GAAS IAA400720710 is acknowledged.

REFERENCES

- [1] C. N. LIKOS, *Phys. Rep.*, **348** (2001) 267.
- [2] F. H. STILLINGER, *J. Chem. Phys.*, **65** (1976) 3968.
- [3] C. N. LIKOS, M. WATZLAWEK, AND H. LÖWEN, *Phys. Rev. E*, **58** (1998) 3135.
- [4] C. MARQUEST AND T. A. WITTEN, *J. Phys. (France)*, **50** (1989) 1267.
- [5] A. MALIJEVSKÝ AND A. SANTOS, *J. Chem. Phys.*, **124** (2006) 074508.
- [6] A. SANTOS, R. FANTONI, AND A. GIACOMETTI, *Phys. Rev. E*, **77** (2008) 051206.
- [7] R. FANTONI, A. GIACOMETTI, A. MALIJEVSKÝ, AND A. SANTOS, *J. Chem. Phys.*, **131** (2009) 124106.
- [8] R. FANTONI, A. GIACOMETTI, A. MALIJEVSKÝ, AND A. SANTOS, *J. Chem. Phys.*, **133** (2010) 024101.
- [9] R. FANTONI, *J. Stat. Mech.*, (2010) P07030.
- [10] P. G. BOLHUIS, A. A. LOUIS, J. P. HANSEN, AND E. J. MEIJER, *J. Chem. Phys.*, **114** (2001) 4296.
- [11] J. MCCARTY, I. Y. LYUBIMOV, AND M. G. GUENZA, *Macromol.*, **43** (2010) 3964.
- [12] L. VEGA, E. DE MIGUEL, L. F. RULL, G. JACKSON, AND I. A. MCLURE, *J. Chem. Phys.*, **96** (1992) 2296.
- [13] E. DE MIGUEL, *Phys. Rev. E*, **55** (1997) 1347.
- [14] F. DEL RÍO, E. ÁVALOS, R. ESPÍNDOLA, L. F. RULL, G. JACKSON, AND S. LAGO, *Mol. Phys.*, **100** (2002) 2531.
- [15] H. LIU, S. GARDE, AND S. KUMAR, *J. Chem. Phys.*, **123** (2005) 174505.
- [16] A. GIACOMETTI, G. PASTORE, AND F. LADO, *Mol. Phys.*, **107** (2009) 555.
- [17] W. KLEIN, H. GOULD, R. A. RAMOS, I. CLEJAN, AND A. I. MEL'CUK, *Physica A*, **205** (1994) 738.
- [18] M. SCHMIDT, *J. Phys.: Condens. Matter*, **11** (1999) 10163.
- [19] B. M. MLADEK ET AL., *J. Phys.: Condens. Matter*, **20** (2008) 494245.
- [20] D. RUELLE, *Statistical Mechanics: Rigorous Results* (Benjamin, London) 1969.
- [21] M. E. FISHER AND D. RUELLE, *J. Math. Phys.*, (1966) .
- [22] D. FRENKEL AND B. SMIT, *Understanding Molecular Simulation* (Academic Press, San Diego) 1996.
- [23] A. Z. PANAGIOTOPOULOS, *Mol. Phys.*, **61** (1987) 813.
- [24] A. Z. PANAGIOTOPOULOS, N. QUIRKE, M. STAPLETON, AND D. J. TILDESLEY, *Mol. Phys.*, **63** (1988) 527.

- [25] B. SMIT, PH. DE SMEDT, AND D. FRENKEL, *Mol. Phys.* , **68** (1989) 931.
- [26] B. SMIT AND D. FRENKEL, *Mol. Phys.* , **68** (1989) 951.
- [27] P. R. TEN WOLDE, M. J. RUIZ-MONTERO, AND D. FRENKEL, *J. Chem. Phys.* , **104** (1996) 9932.
- [28] D. A. KOFKE, *J. Chem. Phys.* , **98** (1993) 4149.